

PREDICTION OF SHIP MANOEUVRABILITY OF AN 8000 TEU CONTAINERSHIP IN DEEP AND SHALLOW WATER: MATHEMATICAL MODELLING AND CAPTIVE MODEL TESTING

Katrien Eloot (Flanders Hydraulics Research, Belgium)

Marc Vantorre (Ghent University, Belgium)

Guillaume Defoortrie (Ghent University, Belgium)

Abstract: The Flemish waterways authorities are permanently concerned about safety of navigation to the Flemish harbours in order to maintain their present position in the European shipping market. Special attention is paid to the effect of the constant growth of ship dimensions, especially in the container trade, on the safety of shipping traffic. Access to and manoeuvring in harbours are characterised by a great diversity of kinematical and control parameters. In 2004-2005 a captive model test program has been executed with a 4.3 m model of an 8000 TEU containership (scale 1:81) combining three distinguished drafts and three under keel clearances from deep to very shallow water. This test program covering all possible combinations of ship velocities and propeller telegraph positions has been used to evaluate hull, propeller and rudder forces to be incorporated in a manoeuvring simulation model applicable in the four quadrants of operation. The influence of combinations of draft and under keel clearance on the first quadrant of operation (forward motion, propeller ahead) will be discussed based on the characteristic dimensions of a turning circle. Sinkage and trim are remarkably influenced by the ship's draft and increase generally with decreasing under keel clearance. The increasing straight-line stability with decreasing ship's draft, especially observed in very shallow water, is probably caused by this squat dependence and the velocity dependent hull force components. Although the rudder is not fully immersed at the smallest draft, differences in rudder forces and correlation parameters are concluded to be small. Finally, as some uncertainties exist about the scale effects, a sensitivity analysis has to be executed in the future to give some insight into the dependence of the mathematical model on individual force components..

1. BACKGROUND ABOUT CONTAINER TRAFFIC TO FLEMISH HARBOURS

Belgium has four major ports of which two of them, the ports of Antwerp and Zeebrugge, accommodate important handling facilities for containerised goods.

The port of Antwerp, one of the most important European ports in the Hamburg-Le Havre range, is accessible through the Western Scheldt, a tidal estuary requiring significant dredging efforts to deepen and maintain the navigation channel. In 1998, a second deepening program 38'-43'-48' was completed which guarantees a tide independent access for ships with drafts up to 11.60 m (38 ft). During the next years a new deepening program will be executed to increase this value to 13.10 m (43 ft). Taking into account that the design draft of the last generation of containerships is 14.5 m, the tidal range has to be used to guarantee the required water depth.

The port of Zeebrugge has several terminals which can handle nearly all types of cargo and corresponding traffic lines (LNG, containers, cars, ro-ro, passengers). Container traffic is of increasing importance; since recently new shipping lines call at

Zeebrugge with vessels up to 8500 TEU.

Taking account of the important role of container traffic for both ports, a thorough knowledge of the behaviour of large container vessels in shallow and restricted waters is required to assess their safety during the approach to and the manoeuvres in the harbours. It is of importance to cover a sufficiently large range of loading conditions, as the draft of container vessels may vary significantly. Moreover, a large range of under keel clearances should be covered, taking account of the tidal range and the local depth variations in the access channels. In the Western Scheldt, for instance, the under keel clearance may vary from 12.5% to more than 100%.

In 2001-2004 an extensive model test program has been executed for the port of Zeebrugge with a fourth generation containership at a draft of 13.5 m to determine ship manoeuvring characteristics. This project focused on the behaviour of container vessels above and in mud layers [1]. Indeed, since its major extension in the 1970s, the outer harbour of Zeebrugge is subject to sedimentation so that permanent maintenance dredging is necessary to keep the port accessible for deep-drafted vessels. As

the bottom is covered with soft mud layers, the boundary between water and bottom is hard to define and the ship behaviour above this “nautical bottom” will change remarkably.

Although the experimental program contained also tests above a hard bottom with different under keel clearances, it was restricted to one draft, so that questions arose about the influence of increasing drafts and/or decreasing under keel clearances (UKC) on ship manoeuvrability. Therefore, a research program was set up by Flanders Hydraulics Research and performed by Ghent University with the objective to examine the manoeuvring behaviour of an 8000 TEU containership at several drafts in deep to very shallow water [2].

2. CAPTIVE MODEL TEST PROGRAM

In 2004-2005 a captive model test program has been executed in the Towing Tank for Manoeuvres in Shallow Water (co-operation Flanders Hydraulics Research – Ghent University) with a 4.3 m model of the containership described in Table 1, combining three distinguished drafts and three under keel clearances (Table 2). The ship model was equipped with a six-bladed propeller ($P/D_p=1.0$ and $A_E/A_0=0.96$) and a rudder with a full scale area of 83 m².

Table 1. Characteristics of an 8000 TEU ship model

	Model scale	Full scale
L_{OA} (m)	4.360	351.96
L_{PP} (m)	4.106	331.76
B (m)	0.530	42.82
T (m)	0.180	14.54
C_B	0.657	
scale	1/80.8	

Table 2 Tested combinations of draft-UKC

	h/T (UKC)		
	2.0 (100%)	1.35 (35%)	1.10 (10%)
14.544	29.09	19.63	16.00
13.5	27.00	18.23	14.85
12.0	24.00	16.20	13.20
T (m full)	h (m full)		

The test program consisted of following test types:

Stationary model tests:

- straight-line tests with positive and negative forward speed;
- oblique towing tests with positive and negative forward speed.

Non-stationary model tests:

- oscillatory tests around ψ -axis;

- harmonic sway tests: pure sway;
- harmonic yaw tests: pure yaw, yaw with drift with positive and negative forward speed;
- multi-modal tests, executed with varying rudder angle, propeller rate or forward speed, while the other parameters are kept at constant values.

The test program for the “deep water” cases (100% and 35% UKC) differs from the one for the “shallow water” condition (10% UKC) in the maximum values applied for forward speed and propeller rpm: the ship velocity was varied between -4 and 16 knots full scale for 100% and 35% UKC and -4 and 10 knots for 10% UKC; the propeller rates ahead were 40, 60 and 80% of the nominal rate n_0 (= 100 rpm full scale) and astern -35, -50 and -80% n_0 . A propeller rpm of 100% n_0 or sea full ahead was only executed during the “deep water” cases.

3. FOUR-QUADRANT MATHEMATICAL MODEL

3.1 Overview

Based on the results of the captive model tests a mathematical model has been developed for each combination of under keel clearance and draft, considering the Froude similarity law. The ship manoeuvring model incorporates the physical background of hydrodynamic forces and has been based on the model as presented in [1]. The hydrodynamic forces induced by hull (H), propeller (P) and rudder (R) are analysed separately and combined in a modular mathematical model by superposition:

$$F = F_H + F_P + F_R \quad (1)$$

The development of the mathematical models is based on a regression analysis using the free “ODRPACK Software for Weighted Orthogonal Distance Regression” [3].

3.2 Hull Forces

The longitudinal hull force X_H , the lateral hull force Y_H and the yawing moment N_H are given by:

$$X_H = (X_{\dot{u}}(u) - m)\dot{u} + mvr + mx_G r^2 + \frac{1}{2} \rho L T \left\{ \begin{array}{l} (u^2 + v^2) X'(\beta) + \left(u^2 + \left(\frac{1}{2} rL\right)^2\right) X'(\gamma) \\ + \left(v^2 + \left(\frac{1}{2} rL\right)^2\right) X'(\chi) \end{array} \right\} \quad (2)$$

$$Y_H = (Y_{\dot{v}} - m)\dot{v} + (Y_{\dot{r}}(\beta) - mx_G)\dot{r} - mur + \frac{1}{2} \rho L T \left\{ \begin{array}{l} (u^2 + v^2) Y'(\beta) + \left(u^2 + \left(\frac{1}{2} rL\right)^2\right) Y'(\gamma) \\ + \left(v^2 + \left(\frac{1}{2} rL\right)^2\right) Y'(\chi) \end{array} \right\} \quad (3)$$

$$N_H = (N_v - mx_G) \dot{v} + (N_r(\beta) - I_{zz}) \dot{r} - mx_G ur + \frac{1}{2} \rho L^2 T \left\{ \begin{array}{l} (u^2 + v^2) N'(\beta) + \left(u^2 + \left(\frac{1}{2} rL \right)^2 \right) N'(\gamma) \\ + \left(v^2 + \left(\frac{1}{2} rL \right)^2 \right) N'(\chi) \end{array} \right\} \quad (4)$$

The drift angle β , the yaw rate angle γ and a drift-yaw correlation angle χ take the velocity effect into account and vary within the range $[-180^\circ; 180^\circ]$.

$$\beta = \text{ATAN2}(-v, u); \gamma = \text{ATAN2}\left(r \frac{L}{2}, u\right) \quad (5)$$

$$\chi = \text{ATAN2}\left(r \frac{L}{2}, v\right)$$

$\text{ATAN2}(y,x)$ is a value in $[-\pi; \pi]$, defined as:

$$\begin{aligned} \text{ATAN2}(y,x) &= \arctan(y/x) && \text{for } x>0 \\ &= \arctan(y/x) + \pi && \text{for } x<0, y>0 \\ &= \arctan(y/x) - \pi && \text{for } x<0, y<0 \\ &= \pm\pi/2 && \text{for } x=0 \end{aligned}$$

3.3 Propeller Induced Forces

3.3.1 Propeller thrust and torque

Captive model tests have been executed in the four quadrants of operation for the speed u and propeller rate n which are defined in Table 3.

Table 3 Definition of the four quadrants of operation

quadrant	U	n	ε (°)
Q1	+	+	[0,90]
Q2	+	-]90,180[
Q3	-	-] -90,0[
Q4	-	+	[-180,-90]

The thrust and torque coefficients for a four-quadrant model are defined as:

$$C_T(\varepsilon) = \frac{T_p}{\frac{1}{2} \rho A_0 [u^2 + (0.7\pi n D_p)^2]} \quad (6)$$

$$C_Q(\varepsilon) = \frac{Q_F}{\frac{1}{2} \rho A_0 D_p [u^2 + (0.7\pi n D_p)^2]} \quad (7)$$

Thrust and torque have been modelled through the wake factor w_p , allowing the calculation of the hydrodynamic advance angle ε :

$$\begin{aligned} \varepsilon &= \text{ATAN2}(u_p, 0.7\pi n D_p) \\ &= \text{ATAN2}(u(1-w_p), 0.7\pi n D_p) \end{aligned} \quad (8)$$

A distinction is made between the wake factor determined according to the thrust identity, w_T , and the torque identity, w_Q . These factors are expressed as function of the apparent hydrodynamic advance angle ε^* :

$$\varepsilon^* = \text{ATAN2}(u, 0.7\pi n D_p) = \text{ATAN2}(J', 0.7\pi) \quad (9)$$

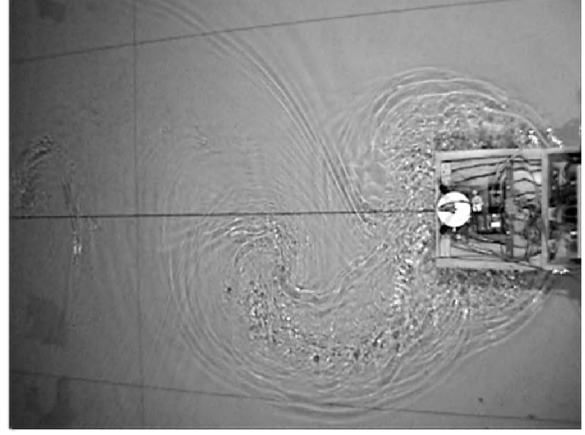


Fig. 1 Large eddies at the aft body during a test ($T=12.0$ m; 10% UKC) with $F_n=0.072$ and $n=-80\% n_0$ (stopping, quadrant 2).

Using equations (6) to (9) a model for the thrust and the torque can be developed:

$$T_p = \frac{0.7^2}{8} \pi^3 \rho n^2 D_p^4 C_T(\varepsilon) (1 + \tan^2 \varepsilon) \quad (10)$$

$$Q_p = \frac{0.7^2}{8} \pi^3 \rho n^2 D_p^5 C_Q(\varepsilon) (1 + \tan^2 \varepsilon) \quad (11)$$

3.3.2 Longitudinal force

The thrust yields a longitudinal force given as:

$$X_p = [1 - t(\varepsilon^*, \varphi^*, \gamma^*)] T_p \quad (12)$$

t being the thrust deduction factor, formulated as a function of the apparent hydrodynamic angles ε^* , φ^* and γ^* , given in expressions (9) and (13).

$$\begin{aligned} \varphi^* &= \text{ATAN2}(v, 0.7\pi n D_p) \\ \gamma^* &= \text{ATAN2}(0.5rL, 0.7\pi n D_p) \end{aligned} \quad (13)$$

3.3.3 Lateral force and yawing moment

The asymmetry of the flow due to propeller action induces a lateral force and yawing moment. The latter are principally stationary in time in the first and third quadrants, but contain an oscillating component in the second and fourth quadrant, with an amplitude which is proportional to the propeller thrust, Fig. 1. Moreover, an additional effect on the hydrodynamic inertia derivatives is observed. Formulations (14) and (15) were used to take these effects into account.

$$Y_p = \frac{n}{n_0} \left(Y_v^n \dot{v} + Y_r^n \dot{r} \right) + T_p(\varepsilon^*) \left[\begin{array}{l} K_1 [Y_{PT}(\beta, \varepsilon^*) + Y_{PT}(\gamma, \varepsilon^*) + \\ K_2 [Y_{PTA}(\beta, \varepsilon^*)] [\cos(\omega(\beta, \varepsilon^*)t + \varphi(\beta, \varepsilon^*))]] \end{array} \right] \quad (14)$$

$$N_p = \frac{n}{n_0} \left(N_v^n \dot{v} + N_r^n \dot{r} \right) + L_{PP} T_p(\varepsilon^*) \left[\begin{array}{l} [N_{PT}(\beta, \varepsilon^*) + N_{PT}(\gamma, \varepsilon^*) + \\ [N_{PTA}(\beta, \varepsilon^*, K_2)] [\cos(\omega(\beta, \varepsilon^*)t + \varphi(\beta, \varepsilon^*))]] \end{array} \right] \quad (15)$$

K_1 and K_2 depend on the quadrant. K_1 is proportional to the forward speed and is taken equal to the Froude number F_n in quadrant 1, and equals 1 in other quadrants; $K_2 = 1$ in quadrants 1, 2, 3 and takes a value between 0 and 1 in quadrant 4, depending on the yaw rate and yaw acceleration.

3.4 Rudder Induced Forces

3.4.1 Rudder dynamics

The ship model was equipped with a single rudder, of which the open water lift and drag characteristics had been determined in a 360 deg range of angles of attack α_R . The non-dimensional drag and lift coefficient are defined as follows:

$$C_D(\alpha_R) = \frac{D_R}{\frac{1}{2}\rho A_R U^2}; C_L(\alpha_R) = \frac{L_R}{\frac{1}{2}\rho A_R U^2} \quad (16-17)$$

D_R being the drag, L_R the lift force, A_R the movable fraction of the rudder area and U the flow velocity. The rudder angle δ_R differs from the angle of attack α_R :

$$\alpha_R = \delta_R + \delta_0 + \beta_R \quad (18)$$

δ_0 , the rudder angle where the normal force F_N vanishes, is a correction for flow asymmetry, with a typical value of +2 deg:

$$\delta_0 = -\delta_R (F_N = 0) \quad (19)$$

In (18), β_R is the local drift angle at the rudder:

$$\beta_R = \text{ATAN2}(-v_R, u_R) \quad (20)$$

u_R , v_R being the longitudinal and transverse component of the flow velocity near the rudder:

$$V_R = \sqrt{u_R^2 + v_R^2} \quad (21)$$

Using expressions (16-21) the forces on the rudder can be calculated:

$$\begin{aligned} F_X &= \frac{1}{2}\rho A_R V_R^2 [C_L(\alpha_R)\sin\beta_R + C_D(\alpha_R)\cos\beta_R] \\ F_Y &= \frac{1}{2}\rho A_R V_R^2 [C_L(\alpha_R)\cos\beta_R - C_D(\alpha_R)\sin\beta_R] \end{aligned} \quad (22)$$

The average or equivalent inflow velocity to the rudder depends on the hull form, which induces wake (in the longitudinal direction) and change of flow direction (in transverse direction), and on the propeller which accelerates the longitudinal flow, depending on the rudder-propeller distance and the rudder area affected by the propeller flow. Generally, the wake at the rudder differs from the wake at the propeller so that a new wake factor has to be introduced. Different wake factors will be derived according to the rudder forces F_X and F_Y to obtain an acceptable accuracy. The water velocity aft of the propeller can be approximated by expressions based on impulse theory. Only the expression for the first quadrant will be presented as discussions in the following chapter will only be based on the ahead motion:

$$u_R = \frac{1-w_R}{1-w_P} \sqrt{\frac{\eta \left[(1-k)\sin\varepsilon + k\sqrt{C_T + \sin^2\varepsilon} \right]^2 + (1-\eta)\sin^2\varepsilon}{\left[(1-w_P)u \right]^2 + \left[0.7\pi m D_P \right]^2}} \quad (23)$$

In (23), η is the propeller diameter to rudder height ratio; k is a factor taking account of the distance rudder-propeller.

It should be noticed that physically more correct alternatives can be formulated for (23); nevertheless, the present approach yields acceptable models.

Although a flow rectification factor is mostly found in literature to take into account the influence of drift and yaw, this factor will be assumed to equal 1 and the wake factor will be considered to depend on the drift and yaw rate angle in a similar way. The sum of both angles is therefore considered. This assumption is acceptable for small drift or yaw rate angles:

$$\frac{v_R}{u} = \frac{v + x_R r}{u} = \frac{v - \frac{1}{2} L r}{u} = -\tan\beta - \tan\gamma \approx -(\beta + \gamma) \quad (24)$$

In this stage, however, $\beta + \gamma$ is used for the whole range.

3.4.2 Rudder induced forces and moment due to correlation

The longitudinal rudder force F_X yields an increase of resistance X_R . Usually the increase will be smaller than F_X , which is modelled as follows:

$$X_R = (1 - t_R) F_X \quad (25)$$

with $t_R > 0$. However, the difference between X_R and F_X seemed insignificant; setting t_R to zero was therefore acceptable.

The asymmetric flow induced by the rudder not only results in a lateral force F_Y on the rudder (with application point x_R), but also in an extra lateral force $a_H F_Y$ (with application point x_H) due to an asymmetric flow around the hull. This leads to:

$$Y_R = (1 + a_H) F_Y \quad (26)$$

The coefficient a_H is a function of ε^* and $\beta + \gamma$ in the first quadrant. The lateral force (26) yields a yawing moment which can be written as:

$$N_R = (x_R + a_H x_H) F_Y \quad (27)$$

The application point x_H can be written as a function of $\beta + \gamma$ in the first quadrant.

3.5 Extrapolation from Model to Full Scale

Scale effects have only been taken into account for the correction of the frictional resistance component in $X'(\beta)$. No other corrections have been performed

although scale effects will probably play a part in all modules of a manoeuvring ship, i.e. hull, propeller and rudder, as has been recognized as a result of a comparative study in [4].

4. DERIVED MANOEUVRING CHARACTERISTICS

4.1 Characteristics of Turning Circles

The turning ability of the 8000 TEU container carrier during a motion ahead will be discussed based on the turning circle characteristics. As this model does not have a known full scale equivalent, lines of existing container vessels not being available, a direct evaluation of the simulated manoeuvring characteristics is impossible. It is known that relatively small differences in geometry, e.g. the aft body, can cause different manoeuvring characteristics. On the other hand, a comparison can be made with the IMO Standards for Ship Manoeuvrability [5] and with full scale trials reported by ship owners of comparable ships. The simulated characteristics of a 35 deg turn performed at design draft with sea full ahead are given in Table 4 for the deep water condition. According to the IMO Standards the tactical diameter should not exceed more than 5 times the ship length. Based on Table 4, it could be concluded that the turning ability of this ship model is only marginally acceptable and the ratios of tactical diameter to ship length are significantly higher than reported values lying in the range between 2.5 and 3.5. This difference could partially be explained based on the larger speed reduction which is observed during full scale manoeuvres compared to the predicted turning manoeuvre.

The influence of draft and available water depth is summarized in Table 5 for the tactical diameter ratio at a telegraph position "half ahead". This reduced propeller rpm is chosen because of the important sinkage that occurs in very shallow water for the lowest draft (see section 4.2). The characteristic dimensions of the turning circle appear to be rather insensitive to the propeller rate.

Table 4 Turning circle characteristics at the design draft and deep water (approach speed 21.6 kts)

	To STBD	To PORT
Advance/ L_{pp}	3.67	3.34
Transfer/ L_{pp}	2.31	2.05
Tact. diameter/ L_{pp}	5.10	4.54
Time to 90°	2'40"	3'00"
Time to 180°	5'34"	6'16"

According to Table 5 the ratios only differ slightly for the different ship's drafts at 100% and 35% UKC, while in very shallow water the tactical diameter at 12 m draft is almost twice the diameter at the design

draft. This remarkable conclusion will be examined in the next sections where force components will be compared and the measured sinkage and trim will be evaluated.

Table 5 Influence of draft and h/T ratio on the ratio of tactical diameter to ship length at telegraph position "half ahead"

		Tactical diameter/ L_{pp}		
		UKC (%)	T=14.5m	T=13.5m
STBD	100	5.08	5.30	5.47
	35	5.12	5.48	5.59
	10	6.64	9.00	12.13
PORT	100	4.55	5.28	4.92
	35	4.77	4.83	5.18
	10	6.85	8.80	10.04

4.2 Squat: Influence of Draft and UKC

The sinkage at the fore (FP) and the aft perpendicular (AP) during a forward motion is presented in Fig. 2 in percentages of the ship's draft as function of the non-dimensional Tuck-parameter, often used in empirical formulae for the prediction of squat (e.g. [6]):

$$\text{Tuck} = \frac{F_{nh}^2}{\sqrt{1 - F_{nh}^2}} \quad (28)$$

F_{nh} is defined as:

$$F_{nh} = \frac{u}{\sqrt{gh}} \quad (29)$$

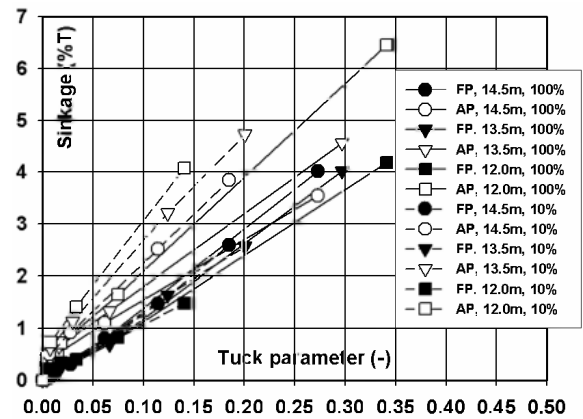


Fig. 2 Sinkage at FP (black) and AP (white) as function of the Tuck parameter: influence of draft T in deep (100% UKC) and very shallow water (10% UKC), $n=80\% n_0$.

Measured sinkage at FP and AP vary almost linearly with the Tuck-parameter and although the variation of sinkage at the FP is almost the same in deep and very shallow water, the sinkage at the AP increases considerably in very shallow water, so that at the largest selected speed the remaining net UKC has been halved. The largest trim is found for the smallest draft. Differences in the force components

and manoeuvring characteristics could therefore probably be explained based on the differences in net under keel clearances which are smaller for the 12.0 m draft compared to the design draft.

4.3 Influence of Draft and UKC on Hull Force Components

4.3.1 Acceleration derivatives

The most important acceleration derivatives, the added mass due to sway and the added moment of inertia due to yaw, are presented in Fig. 3 and Fig. 4. These derivatives only play a part during the initial phase of the turning manoeuvre and do not affect the stationary turning phase. Both derivatives are made non-dimensional based on the ship's mass and presented as functions of the ship length to under keel clearance ratio, $L/(h-T)$. It should be borne in mind that the *absolute* under keel clearance $h-T$ decreases – and the parameter $L/(h-T)$ increases – with decreasing draft if the *relative* under keel clearance, expressed as a percentage of draft, is kept constant. The magnitude of the non-dimensional inertia derivatives increases as well for a decreasing draft at constant relative UKC.

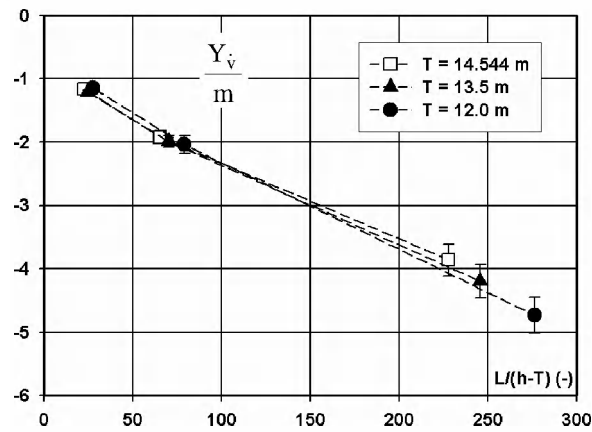


Fig. 3 Influence of draft and $(h-T)$ on the added mass due to sway.

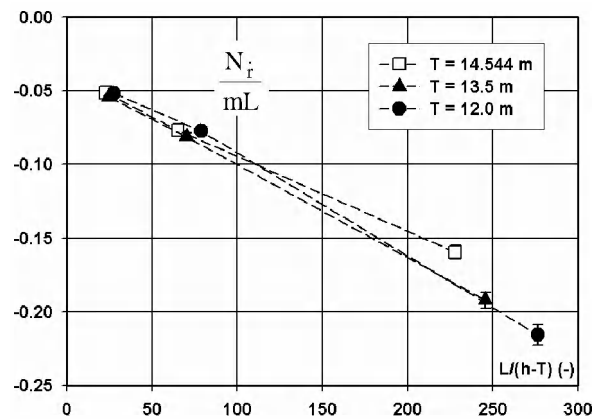


Fig. 4 Influence of draft and $(h-T)$ on the added moment of inertia due to yaw.

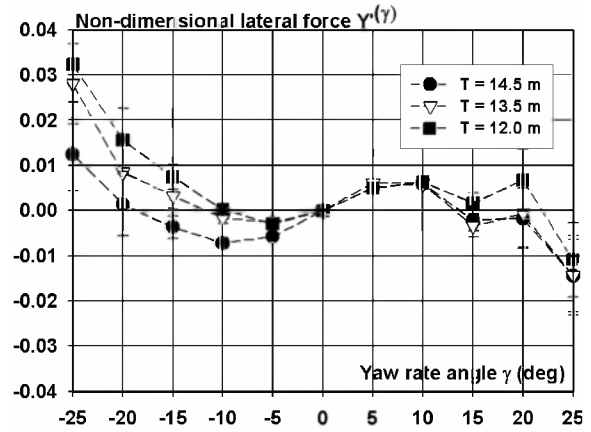


Fig. 5 Influence of draft on non-dimensional lateral force due to yaw in deep water (100% UKC).

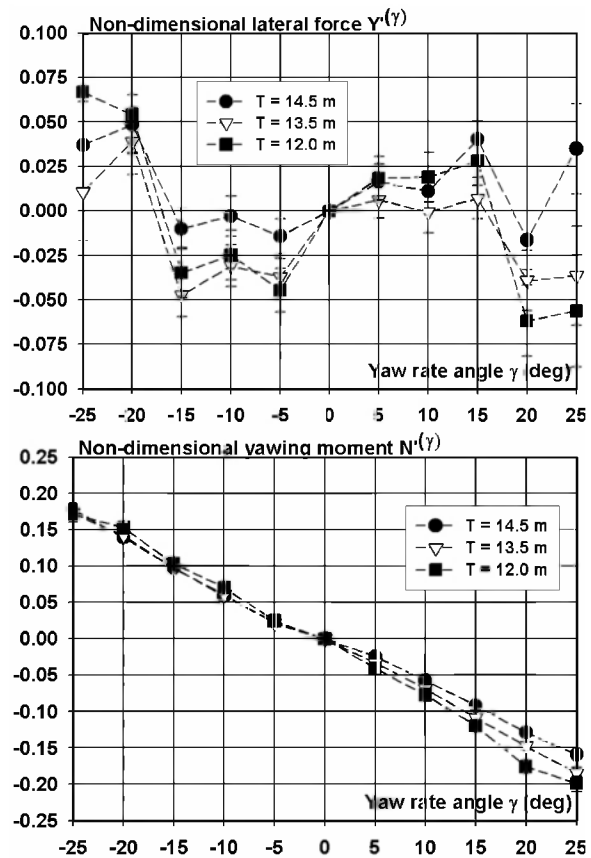


Fig. 6 Influence of draft on non-dimensional lateral force and yawing moment due to yaw in very shallow water (10% UKC).

The increase of $|Y_v / m|$ and $|N_r / mL|$ with decreasing draft can partially be ascribed to the decrease of the ship's mass, at least in the very shallow water case. In deeper water, on the contrary, the non-dimensional acceleration derivatives remain nearly constant with varying draft.

4.3.2 Velocity dependent terms

The velocity dependent lateral forces and yawing moments are directly linked to the stability levers Γ_v and Γ_r which determine the straight-line stability of a

ship [7]:

$$l'_v \equiv \frac{N'_v}{Y'_v} < \frac{N'_r}{-m'+Y'_r} \equiv l'_r \quad (30)$$

Due to the increasing dynamic stern trim with decreasing draft, the lever l'_v is expected to move aft so that the ship will become more stable, giving larger values for turning circle characteristics such as the tactical diameter.

Based on Fig. 5 and Fig. 6, the following may be concluded:

- Although turning circle characteristics based on full scale trials show only a small asymmetry between a port and a starboard turn, lateral force and yawing moment due to sway or yaw are not necessarily anti-symmetrical. A clarification for this asymmetry needs further examination.
- The influence of the ship's draft on these forces is not straightforward for positive or negative angles β or γ at a constant UKC. For 10% UKC as an example, the influence of draft on yawing moment $N'(\gamma)$ is limited for negative yaw rate angles (turn to port) while it is noticeable for positive angles. The important asymmetry between a port and a starboard turn for the smallest draft at 10% UKC compared to the other drafts, could partially be explained based on these test results with a larger $|N'(\gamma)|$ value for 12.0 m draft and positive yaw rate angles.
- The errors on the lateral force due to yaw, $Y'(\gamma)$, are large especially in shallow water and in deep water for larger yaw rate angles. The influence of a modification of this table based on the uncertainty will be subjected to a sensitivity analysis as was performed in [8].

4.4 Influence of Draft and UKC on Propeller Coefficients

For the first quadrant of operation the major contribution of the propeller is based on the propeller thrust yielding the propeller induced longitudinal force X_P . The propeller induced lateral force and yawing moment are of minor importance.

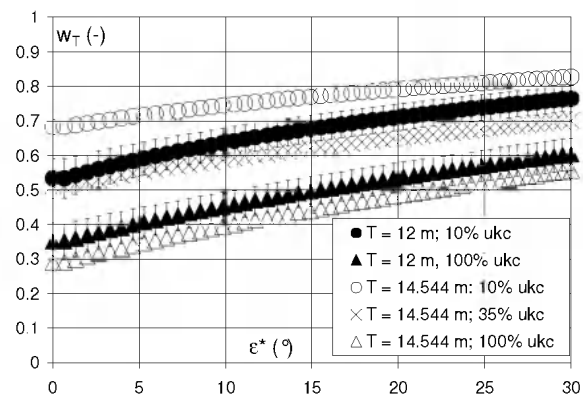


Fig. 7 Modelled wake fraction w_T as function of the apparent advance angle ϵ^* .

For several conditions, the wake factor w_T according to thrust identity is shown in Fig. 7. For a constant draft the wake factor decreases with increasing water depth as the inflow into the propeller resembles more and more the free stream condition. The influence of ship's draft for different UKCs is not straightforward. In deep water the wake factor at the smallest draft is somewhat larger than the factor for the design draft while at 10% UKC the opposite is found. In very shallow water, the inflow velocity into the propeller will therefore be higher for 12 m draft compared to 14.5 m draft, giving a smaller propeller thrust at the smallest draft.

4.5 Influence of Draft and UKC on Rudder Induced Forces

At the smallest ship's draft of 12.0 m the rudder area is not fully immersed so that smaller rudder forces could be expected. A comparison of measured longitudinal and lateral rudder forces shows nevertheless that this is not necessarily true.

In Fig. 8 the difference in F_X for a rudder angle to port (>0) and both ship's drafts is small while for a rudder angle to starboard the additional resistance force F_X is smaller in magnitude for the smallest draft. The speed reduction will therefore be smaller resulting in a turning circle with larger characteristic dimensions compared to the design draft.

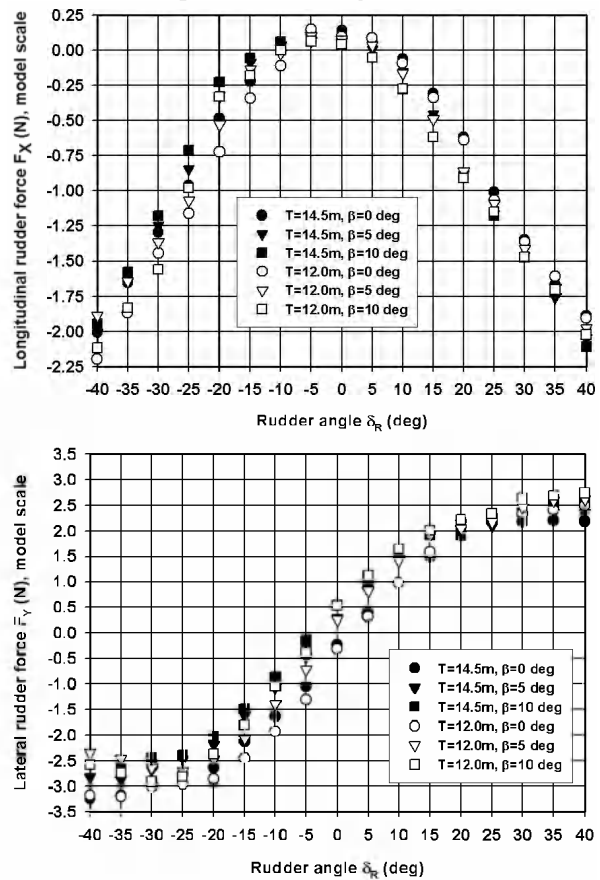


Fig. 8 Comparison of measured force F_X and F_Y at drafts of 12.0 and 14.5 m full scale ($F_n=0.072$, $n=60\%n_0$, 10% UKC).

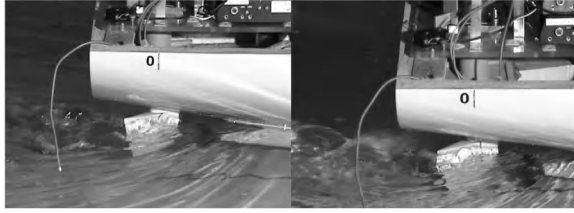


Fig. 9 Flow at the rudder at 100% (left) and 10% (right) UKC for a full scale draft of 12 m.

For the lateral rudder force F_Y , differences are also more pronounced for a starboard than for a port rudder command. Especially for negative rudder angles, the magnitude of the rudder force F_Y depends on the applied rudder angle: at smaller rudder angles ($\delta_R \leq -20^\circ$), higher rudder forces are measured for the smallest draft, while at hard starboard rudder, the rudder force appears to be slightly higher if the ship is loaded at her design draft.

Despite of the difference in immersed rudder area for the three drafts, the small difference in forces at the rudder position could be explained based on the important increase of the flow induced by the wake and the propeller slipstream for the ship model loaded at the smallest draft as shown in Fig. 9.

Lateral forces F_Y measured during low speed model tests, characterized by large ranges of drift angles, are presented in Fig. 10. The influence of ship's draft is small with somewhat larger values for the 12.0 m draft at high rudder angles.

Differences in the correlation coefficients due to rudder action are examined for the hull coefficient a_{H1} (Fig. 11) and the application point x'_{H1} (Fig. 12). Depending on the apparent advance angle, an increase of draft may lead to either smaller or larger values for the hull coefficient a_{H1} . The ship self-propulsion point corresponds to an advance angle ϵ^* of approximately 20 deg so that higher a_{H1} values are found for the design draft compared to the smaller drafts; for lower advance angles or higher propeller loading the additional hull contribution is larger for the smallest draft compared to the others.

Some doubt may arise about the accuracy of this coefficient for advance angles ϵ^* higher than 15 deg: these values are dominating the simulation runs in Table 5 while they can only be obtained during the model tests in very shallow water using low propeller rates due to the limited model speed. Generally, a higher hull coefficient a_{H1} causes an increased turning ability.

The application point x'_{H1} of the additional hull contribution to the rudder action is shown as function of the water depth to draft ratio in Fig. 12 for a straight ahead motion. This point moves towards midships with decreasing UKC. The influence of ship's draft is not clear, although the differences for each UKC are limited. The reduced turning ability in

shallow water can partially be explained based on the reduced lever x'_{H1} .

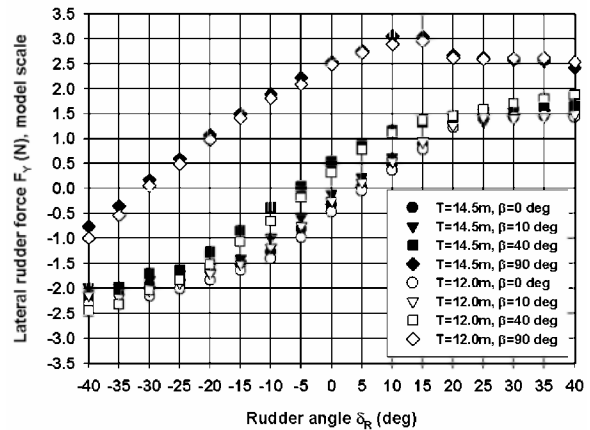


Fig. 10 Comparison of measured force F_Y at drafts of 12.0 and 14.5 m full scale ($F_n=0.018$, $n=60\%n_0$, 10% UKC).

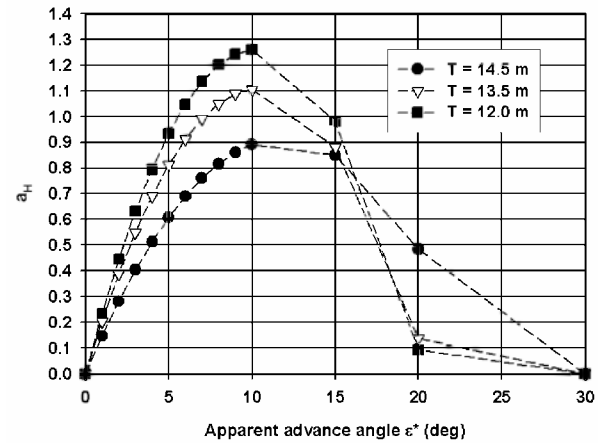


Fig. 11 Influence of ship's draft on correlation factor a_{H1} (straight ahead, 10% UKC)

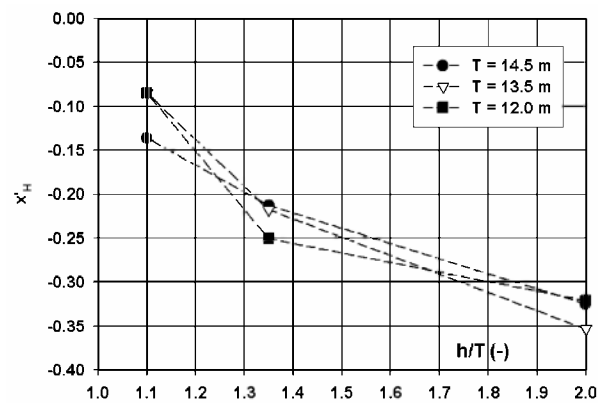


Fig. 12 Influence of ship's draft and UKC on the application point x'_{H1} (straight ahead)

5. CONCLUSION

A clear influence of ship's draft or loading condition on ship manoeuvrability in both deep and very shallow water is seldom found in literature. Full scale

trials at the delivery often provide manoeuvring characteristics in a trimmed ballast condition or even keel design condition, with mostly only deep water. This research was set up to meet this lack of knowledge. Thanks to the extensive program of captive model tests, available in the four quadrants of operation, a mathematical manoeuvring model is developed with a wide applicability. Only the turning ability in the first quadrant is discussed here and the conclusions are:

- Sinkage and trim are remarkably influenced by the ship's draft. Generally, squat increases with decreasing UKC while the sinkage at the aft perpendicular is much larger for an intermediate draft compared to the design draft.
- The characteristic dimensions of a turning circle differ only slightly for all drafts in deep (100% UKC) and shallow water (35% UKC). In very shallow water, the tactical diameter ratio for 12.0 m draft is almost twice the ratio for the design draft. In addition, differences between a port and a starboard turn increase with decreasing UKC.
- The non-dimensional added mass due to sway $|Y_{\dot{v}}/m|$ and the added moment of inertia due to yaw $|N_{\dot{r}}/mL|$ are nearly constant in deep water while these non-dimensional derivatives increase with decreasing draft in very shallow water. This increase can partially be ascribed to the decrease of the ship's mass.
- The increasing straight-line stability with decreasing ship's draft can be explained by the evolution of the velocity dependent hull force components. As an example, the yawing moment due to yaw $|N'(\gamma)|$ increases with decreasing draft for positive yaw rate angles in very shallow water. The larger asymmetry between a port and starboard turn at 10% UKC and 12.0 m draft could be explained based on this difference.
- The lack of anti-symmetry of the modeled velocity dependent lateral force and yawing moment as functions of drift angle or yaw rate angle needs further examination.
- Although the rudder is not fully immersed at 12.0 m draft the forces measured at the rudder only differ slightly for the different drafts. Even the difference for the correlation parameters a_H and x'_H is small so that the decreasing turning ability with decreasing draft in very shallow water cannot be explained based on these results.
- Due to the difference in squat, especially in very shallow water, the test program for the smallest draft and the other drafts was not identical. Some tests could not be executed, which could have

affected the derived mathematical model.

- As some uncertainties still exist about the scale effects that must be taken into account in deep and shallow water, a sensitivity analysis of individual model components could give more insight into the relationship between math model and resultant full scale manoeuvring characteristics.

REFERENCES

- [1] Delefortrie G., Vantorre M., Eloot K. "Modelling navigation in muddy areas through captive model tests", *Journal of Marine Science and Technology*, Vol. 10 (4), pp. 188-202, 2005
- [2] Vantorre M., Eloot K. et al "Wetenschappelijke bijstand voor het uitvoeren van proeven en het opstellen van wiskundige manoeuvreermodellen voor 8000 TEU containerschepen voor de toegang tot de Vlaamse havens", overeenkomst 16EB/04/02, 2004
- [3] Boggs P.T., Byrd R.H., Rogers J.E., Schnabel R.B. "User's Reference Guide for ODRPACK Version 2.01 Software for Orthogonal Distance Regression", Center for Computing and Applied Mathematics, U.S. Department of Commerce, 1992
- [4] 24th International Towing Tank Conference, The Manoeuvring Committee "Final report and recommendations to the 24th ITTC", Southampton, 2005
- [5] International Maritime Organization, Maritime Safety Committee "Explanatory notes to the Standards for ship manoeuvrability", Resolution MSC.137(76), 2002
- [6] Ankudinov V., Daggett L.L., Hewlett J.C., Jakobsen B.K. "Prototype measurement of ship sinkage in confined water" *Proceedings of MARSIM2000*, Orlando, pp. 233-247, 2000
- [7] 23rd International Towing Tank Conference, The Manoeuvring Committee "Final report and recommendations to the 23rd ITTC", Venice, 2002
- [8] Martinussen K., Ringen E. "Manoeuvring Prediction During Design Stage" *International Workshop on Ship Manoeuvrability at the Hamburg Ship Model Basin*, paper No. 8, 2000

AUTHOR'S BIOGRAPHY

Katrien Eloot obtained a Master's degree in Naval Architecture from Ghent University Belgium in 1995. She worked as an academic assistant at the university from 1995 until 2000. There she started her principal research concerning mathematical modeling of ship manoeuvres in shallow water and captive model testing. In 2001 she entered her present post at Flanders Hydraulics Research, a laboratory of the Flemish Community. As study-engineer she carries out research contracts on real-time and fast-time manoeuvring simulation for the public and the private sector.

